

# Arrhythmia in the Amazon: La Niña influence on riverine organic molecular signatures

**Martin Kurek** (✉ [mrk19f@my.fsu.edu](mailto:mrk19f@my.fsu.edu))

Florida State University

**Aron Stubbins**

Northeastern University <https://orcid.org/0000-0002-3994-1946>

**Travis Drake**

Department of Environmental Systems Science, Swiss Federal Institute of Technology

<https://orcid.org/0000-0002-7564-974X>

**Jose Mauro Moura**

Center for Interdisciplinary Formation, Federal University of Western Para <https://orcid.org/0000-0003-4962-8870>

**Robert Holmes**

Woods Hole Research Center

**Helena Osterholz**

Marine Chemistry, Leibniz Institute for Baltic Sea Research

**Thorsten Dittmar**

Carl von Ossietzky University of Oldenburg <https://orcid.org/0000-0002-3462-0107>

**Bernhard Peucker-Ehrenbrink**

Woods Hole Oceanographic Institution

**Miyuki Mitsuya**

Center for Interdisciplinary Formation, Federal University of Western Para

**Robert Spencer**

Florida State University

---

## Article

**Keywords:** Amazon, El Niño, Arrhythmia, organic matter

**Posted Date:** September 10th, 2020

**DOI:** <https://doi.org/10.21203/rs.3.rs-57049/v1>

**License:** © ⓘ This work is licensed under a Creative Commons Attribution 4.0 International License.

[Read Full License](#)

# Abstract

As climate-driven El Niño Southern Oscillation (ENSO) events are projected to increase in frequency and severity, much attention has focused on impacts regarding ecosystem productivity and carbon balance in Amazonian rainforests, with little attention given to carbon dynamics in fluvial ecosystems. We compared the wet 2012 La Niña period to the following normal hydrologic period in the Amazon River. Elevated water flux during the La Niña was accompanied by dilution of inorganic ion concentrations. Furthermore, the La Niña period exported 2.77 TgCyr<sup>-1</sup> more dissolved organic carbon (DOC) than the normal period, an increase greater than annual Mississippi River DOC export. Using ultra-high-resolution mass spectrometry, we detected both seasonal and inter-annual variations in dissolved organic matter (DOM) compositions, revealing that DOM exported during the dry season and the normal period was more aliphatic, whereas compounds in the wet season and following the La Niña event were more aromatic, with ramifications for its environmental role. Furthermore, compounds were highly correlated to a 6-month lag in Pacific temperature and pressure anomalies, demonstrating that ENSO events impact DOM compositions exported to the Atlantic Ocean.

# Main Text

Inland waters have been increasingly recognized as hotspots for global carbon cycling, moving away from being viewed as passive transporters and reservoirs, to being accepted as interwoven conveyers and reactors<sup>1-4</sup>. Dissolved organic matter (DOM) is a major component of freshwater carbon dynamics and represents a complex mixture of molecules from various terrestrial and aquatic sources with many ecosystem functions, ultimately serving as one of the most important intermediaries in the global carbon cycle<sup>2</sup>. The reactivity or persistence of DOM is related to both the local environmental conditions and its intrinsic chemical composition<sup>5-9</sup>. Ultra-high-resolution Fourier transform-ion cyclotron resonance mass spectrometry (FT-ICR MS) has been adopted in recent years as the most comprehensive technique for characterizing DOM composition as well as linking this to lability, revealing potential sources and degradation processes within heterogenous mixtures<sup>9-13</sup>. Many of these compositional differences are driven by *in situ* processing during riverine transport<sup>5,10,14</sup>, which is responsible for both producing new compounds and mineralizing DOM to CO<sub>2</sub>, and linking terrestrial carbon to the atmospheric and marine reservoirs<sup>2,4,15-16</sup>. Riverine export of DOC is approximately 250 Tg C annually, and provides the largest flux of reduced carbon from terrestrial to marine environments<sup>15</sup>, with the Amazon River responsible for over 10% of the land-ocean DOC flux<sup>17-19</sup>.

The Amazon is the largest river on Earth by discharge and drainage area, contributing almost 20% of the global riverine discharge to the ocean and draining a massive basin of over 6x10<sup>6</sup> km<sup>2</sup><sup>19</sup>. The Amazon River transports inorganic solutes, which are diluted with increasing discharge, and biogenic solutes, which are enriched with discharge; the so-called “rhythm” of the Amazon<sup>17,20-21</sup>. Among the biogenic solutes, DOM is transported from the high Andes, grasslands, forests, and floodplains, and continually processed on the journey to the Atlantic Ocean<sup>22-25</sup>. Though the fate of the DOM varies, the majority is

thought to be directly exported into the Amazon River coastal plume downstream<sup>26-27</sup>, whereas the more photo- and biolabile compounds are thought to be mineralized instream<sup>6,24,28</sup>. Given that the Amazon River outgasses 0.47-1.4 Pg C year<sup>-1</sup> as CO<sub>2</sub> to the atmosphere<sup>29-30</sup>, the high DOC concentrations of its tributaries<sup>18</sup> and the microbial preference to respire biolabile DOM<sup>31-32</sup>, it's likely that a portion of Amazon riverine DOM contributes to CO<sub>2</sub> fluxes<sup>24,33</sup>.

Changes in climate and land use are expected to alter the feedback between atmospheric and aquatic carbon export from the Amazon Basin<sup>16</sup>. Periodic anomalies in Pacific sea surface temperatures and air pressures result in events known as the El Niño Southern Oscillation (ENSO), where warmer temperatures are termed El Niño years and colder periods are La Niña years. Historical trends suggest that La Niña events contribute to colder and wetter conditions in the Amazon Basin, while El Niño events lead to warmer and drier conditions<sup>34-35</sup>; both expected to increase in severity and frequency from climate change<sup>36-37</sup>. These variations in precipitation have resulted in regional flooding and droughts across the Amazon Basin<sup>38-39</sup>, which influence the annual discharge of the mainstem<sup>34-35,40</sup>. While multi-year Amazon River DOC fluxes have been assessed<sup>17-18</sup>, DOM compositions have been limited to discrete sampling campaigns with incomplete seasonal coverage<sup>12,25-27</sup> and have been hypothesized not to vary with discharge<sup>41</sup>. Furthermore, the effects of ENSO on inter-annual variability in riverine DOM have not been examined. Thus, this is the first study to investigate DOM compositions from the Amazon River spanning an ENSO event. Specifically, we compare DOC fluxes and DOM properties between a La Niña and non-ENSO period (normal period).

### ENSO-driven changes in Amazon hydrology and export

Monthly Amazon River sampling began during the onset of the 2011-2012 La Niña whose impacts could be seen at the furthest downstream gauging station and our sampling site in Óbidos, Brazil (Figure 1A). La Niña events were characterized by Oceanic Niño Index (ONI) values below -0.5, which has been utilized by NOAA to predict the severity of ENSO using temperature anomalies in the east-central Equatorial Pacific (Figure 1A). The ONI in this study also closely follows the Southern Oscillation Index (SOI) (Figure S1A,B), which is used as an indicator for ENSO developments calculated by sea-level atmospheric pressure differences between Darwin, Australia and Tahiti, French Polynesia. The La Niña event resulted in early and widespread precipitation across the Northern and Western Amazon Basin starting in late 2011 with record flooding occurring in the tributaries feeding into the Amazon mainstem, while other regions received normal or even less rainfall<sup>38-39</sup>. La Niña peak discharge at Óbidos in mid-May (~270,000 m<sup>3</sup>s<sup>-1</sup>) was higher and nearly two weeks earlier than in the previous and following years. Following the wet season, precipitation and discharge patterns returned to normal (defined as non-ENSO, -0.5<ONI<0.5) until the end of 2013 (Figure 1A). Thus, two distinct hydrological regimes spanned the course of the study; the anomalous wet period influenced by the La Niña event (La Niña year) and the following period (normal year). The La Niña year started from August 2011 to July 2012 with a discharge flux of 5,849 km<sup>2</sup>yr<sup>-1</sup> (Figure 1, green region) and the following normal year was from August 2012 to July

2013 with a discharge flux of  $5,578 \text{ km}^2\text{yr}^{-1}$  (Figure 1, blue region). This division was chosen for two reasons. First, samples from mid 2011 to late 2013 were separated into two equivalent hydrologic years, starting and ending on the falling limb of the hydrograph such that any differences between the years would be attributed to inter-annual variations and not seasonal variations. Second, correlations between discharge and ENSO indices are not instantaneous and are detected in Óbidos after a 6-month lag from the SOI<sup>34,40</sup> (Figure S1A) as well as the ONI (Figure S1B). By February 2012, ONI values had increased ( $>-0.5$ ), signifying the end of a moderate La Niña period in the Pacific, but the effects on discharge at Óbidos would still occur for about 6 months. Therefore, the discharge period after July 2012 would no longer have been influenced by the La Niña event and was denoted as the start of the normal year.

The distinction between the years was confirmed using geochemical measurements from the Amazon mainstem at Óbidos. Major dissolved inorganic ions ( $\text{Cl}^-$ ,  $\text{SO}_4^-$ ,  $\text{Ca}^{2+}$ ,  $\text{Mg}^{2+}$ ,  $\text{Na}^+$ ,  $\text{K}^+$ ) sourced primarily from the Andes<sup>21</sup> displayed predictable seasonal variability with higher concentrations in the dry period and lower concentrations in the wet period due to dilution<sup>20-21</sup> (Figure 1B; Supplemental methods). However, monthly concentrations during the low discharge period were attenuated during the La Niña year (Figure 1B) indicating greater dilution from the widespread precipitation that occurred in the Northern and Western sub-basins at that time<sup>38</sup>. Average  $\text{SiO}_2$  concentrations were also significantly higher during the normal year ( $9.94 \pm 1.96$  vs  $8.02 \pm 0.23 \text{ mgL}^{-1}$ ,  $p=0.006$ ; Figure 1C) reflecting the greater proportion of Andean water passing through Óbidos during the La Niña and diluting locally weathered Si from lower Amazon reaches<sup>20-21</sup>. While the inorganic solute concentrations are controlled by dilution, biogenic solute concentrations typically correlate positively with discharge in terrestrial riverine systems<sup>8,42</sup>. Indeed, DOC concentrations increased with discharge at Óbidos (Figure 1D), likely driven by greater overland flow and input of terrestrial DOM from surface litter and organic soil horizons<sup>19,42</sup>. Average DOC concentrations between the years did not differ significantly, which is typical of the stable DOC concentrations in the mainstem<sup>17,25</sup>. However, the flux of DOC from the Amazon was  $\sim 10\%$  higher in the La Niña year (26.86 Tg C) than in the normal year (24.09 Tg C) by  $2.77 \text{ Tg C yr}^{-1}$ , amounting to additional DOC export greater than from the Mississippi River each year<sup>8</sup>.

### Seasonal trends in Amazonian DOM composition

Wet season DOM contained compounds that were of higher molecular weight (MW), more oxidized, and aromatic than in the dry season which were lower MW, reduced, and more aliphatic (Figure 2A,B,C). These compositional differences can be interpreted in the context of bioavailability for heterotrophs because smaller, reduced, and aliphatic compounds are typically more biolabile, whereas larger, aromatic, and oxygenated compounds are usually more stable on the timescales considered here<sup>13,43</sup>. These trends are consistent with previous Amazonian DOM compositions from Óbidos<sup>25</sup> as well as from other major tropical<sup>44</sup> and arctic<sup>45-46</sup> rivers, with their diverse compositions suggesting heterogeneous sources. Riverine aromatic and oxygenated compounds typically originate from organic soil horizons and fresh plant litterfall that are mobilized during periods of increased hydrological

connectivity, whereas microbial DOM is leached from deeper subsurface soil and groundwater under baseflow<sup>47-48</sup>. Consequently, DOM during seasonal high-discharge events is exported to the ocean with a greater relative contribution from the molecular “island of stability” (IOS) that has been suggested to persist for tens of thousands of years in marine DOM<sup>11</sup>(Figure 2D). Although IOS compounds were more abundant during high discharge events (Figure 2D), they were still relatively minor compared to the IOS content of marine DOM, and DOM from a variety of global rivers<sup>9</sup>. Given that IOS content has shown to be inversely proportional to  $\Delta^{14}\text{C}$ <sup>9</sup>, this supports the dominance of modern and fresh DOC exported by the Amazon<sup>33</sup>. During low flow periods, the IOS fraction decreases, at which time more biolabile compounds from groundwater and algal inputs have been suggested to support microbial respiration within the Amazon River<sup>17,22,24</sup>. However, the increase in biolability is likely small given the overall stable nature of Amazon DOM, which has undergone upstream processing<sup>28</sup>. Thus, predictable variations in seasonal hydrology offer a reasonable justification for the yearly DOM compositions at Óbidos, which had not been expected to vary with discharge<sup>41</sup>.

### Interannual variability in Amazonian DOM composition

Despite the supposed annual stability of Amazon River DOM, the difference in discharge between the years ( $271 \text{ km}^2\text{yr}^{-1}$ ) was accompanied by shifts in the downstream molecular DOM properties. In the La Niña year, DOM was significantly ( $p < 0.05$ ) larger, more aromatic, oxygenated, and had less S and P-containing compounds than in the normal year (Figure 2, Table S1). Additionally, the average proportion of IOS compounds was significantly higher in the La Niña year (6.0%) than in the normal year (4.8%), but average N/C ratios remained unchanged (Figure 2, Table S1). These changes suggest that the La Niña event mobilized DOM of more terrestrial character into the Amazon River, and subsequently exported to the Atlantic Ocean, than during the normal year. A Jaccard dissimilarity matrix of all the samples indicated that during the normal year, DOM from the dry and wet seasons were distinct, each clustering separately (Figure 3A) as is expected by the mobilization of heterogeneous sources<sup>44-47</sup>. In contrast, DOM compositions across the entire La Niña year (2011 to July 2012) were homogenous and did not follow this normal year trend, instead resembling wet season DOM from the normal year (Figure 3A). Additionally, the La Niña-driven DOM contained many compounds that were absent from the following year, as illustrated by its high dissimilarity to the group of common molecules found in all the Amazon samples (Figure 3B). Generally, this percent dissimilarity is analogous to chemodiversity, determined from molecular richness, and follows the normal year hydrograph (Figure 3B). However, it remained constant during the La Niña year (Figure 3B), effectively skipping a natural seasonal beat (i.e. arrhythmia) in Amazonian DOM export.

Although the 6-month lag period is strongly supported by the discharge, DOC flux, and inorganic ion data (Figure 1), we further investigated various lag periods on the DOM composition at Óbidos to confirm the separation between the years. Relative intensities of all molecular formulae from the Amazon River were regressed against ONI values ranging from a 0 to 12-month lag period, where a 0-month lag period was just the ONI values measured the same month that DOM was sampled and a 12-month lag

period included ONI values measured 12 months prior to DOM sampling. The number of significantly correlated ( $p < 0.05$ ) molecular formulae was lowest at 0 months (233) and peaked (3,537) at a 6-month lag period before decreasing through 12 months (850) (Figure 4A). A similar pattern was observed by correlating formula intensities using the SOI-lagged values, which also peaked at 6 months (Figure S2A); illustrating the utility of both indices to predict changes in Amazon River DOM composition. DOM correlations with 6-month lagged ONI values followed compositional patterns driven by hydrology (Figure 4B). Compounds that correlated positively with the ONI (red points, Figure 4B) were more abundant during normal (non-ENSO) conditions and were more saturated and oxygen-deficient than La Niña DOM, suggesting greater biolability<sup>13,43</sup>. In contrast, formulae correlated negatively with the ONI (blue points, Figure 4B), meaning they were more abundant during La Niña, were highly aromatic and oxygenated reflecting their presumed terrestrial origins<sup>13,43</sup> and suggestive of greater photolability and hydrophilicity<sup>10,13</sup>. An analogous trend was observed with 6-month lagged SOI correlations, though the correlations were inverted since La Niña events are indicated by positive SOI values (Figure S2B).

### Implications of future ENSO events on Amazonian DOM export and carbon cycling

The composition of Amazon DOM is highly dependent on how La Niña, and other ENSO events, influence each region within the basin and subsequently, the DOM exported from each tributary. For instance, heavy precipitation during the La Niña was focused mostly in the Northern and Western sub-catchments, as has typically occurred in past La Niña events<sup>38-39</sup>. The Northern regions drain into the mainstem via the blackwater Rio Negro and the western regions feed the whitewater Rio Solimões. These tributaries join upstream of Óbidos, together contributing the majority of DOC in the Amazon River<sup>18</sup>. The Rio Negro exports predominantly aromatic and polyphenolic compounds into the mainstem, while whitewater tributaries adsorb this material to their sediment load upon mixing and contribute relatively more aliphatic compounds<sup>12</sup>. However, different precipitation patterns could alter the proportion and composition of DOM exported from each tributary. For example, greater precipitation in the Rio Negro Basin and Northeast alone would have leached more aromatic DOM into the tributary from organic-rich soils, possibly overwhelming the adsorptive capacity of fine suspended sediment from the Solimões<sup>12,49</sup>, resulting in even more aromatic and IOS compounds exported to the mainstem. In contrast, had the La Niña caused more precipitation in the south than the north, fine suspended sediment from the Peruvian and Bolivian Andes might have adsorbed more aromatic DOM from the Rio Negro as the tributaries mixed, lowering the aromaticity and nitrogen content of the DOM in the Amazon River<sup>7,23,49</sup>. Thus, the extent and location of precipitation anomalies within the Basin determine the sources and quality of DOM exported from the tributaries into the mainstem, which could subsequently impact the rate of mineralization in the Amazon and its fate in the Atlantic Ocean.

The Amazon River emits vast amounts of CO<sub>2</sub> to the atmosphere<sup>29-30</sup> with annual fluxes potentially susceptible to changes in climate and land use<sup>16</sup>. We propose that DOM compositions exported from the Amazon River will vary with future ENSO cycles, which are expected to increase in frequency and intensity this century from anthropogenic climate change<sup>36-37</sup>. More frequent La Niña events will likely result in

greater riverine discharge at Óbidos<sup>34-35</sup>, exporting more terrestrial aromatic DOM into the Atlantic Ocean with a lower potential for microbial mineralization during transport and in the river plume. However, this may also lead to greater photooxidation of DOM, which is typically only a minor source of CO<sub>2</sub> in the Amazon Basin<sup>6,50</sup>, but is an important degradation process for organic-rich waters particularly in coastal ecosystems and in the Amazon plume<sup>10,26-27</sup>. In contrast, more frequent El Niño events may export less terrestrial DOM into the Amazon River as a result of less regional rainfall and reduced hydrologic connectivity<sup>34-35</sup>, with its own unique arrhythmia and opposite molecular trends of what was observed during the La Niña year (Figure 1). Given that past ENSO-related revents have been linked to predictable changes in the Amazon carbon balance<sup>34</sup>, it is likely that future events may also influence regional carbon cycling. Overall, we hypothesize that ENSO-related events will increase arrhythmic variations in exported DOM compositions and will impact future CO<sub>2</sub> fluxes from the Amazon River, possibly increasing  $p\text{CO}_2$  from respiration of mobilized DOM compounds<sup>31-32</sup>.

Though the long term effects of ENSO on Amazonian carbon balance currently remains speculative, the differences in DOC fluxes and DOM composition observed between a La Niña and a normal year along with the projected increase in ENSO events suggest that discharge, DOC, and CO<sub>2</sub> fluxes must be continually reevaluated in long-term datasets to better understand their contributions to the global carbon cycle. This includes considerations as to where studies will be conducted within the basin since tributaries export DOM from various sources and may not all be equally mobilized by ENSO events.

## Methods

### Study site and sampling:

Near-monthly water sampling from July 22, 2011 to November 16, 2013 was conducted in the Amazon mainstem at the furthest downstream Brazilian National Water Agency (<https://www.ana.gov.br>) gauging station (17050000) at Óbidos (1°56'S 55°30'W), where over 90% of the DOC flux of the Amazon to the Ocean is captured<sup>19</sup>. During each sampling date, three water samples (1 L) were collected at 0.5 m depth from the river at the gauging station across the channel in equal spacing. The samples were combined into a 4 L carboy to make a composite sample and filtered through a 0.45 µm capsule filter using a peristaltic pump and tubing into polycarbonate bottles. The filtered samples were immediately frozen and kept in the dark until analysis. River discharge measurements were taken from the gauging station the same day as water samples.

Monthly values for the Southern oscillation index (SOI) were obtained from the Australian Government Bureau of Meteorology<sup>51</sup> and values for the Oceanic Niño index (ONI) were obtained from the National Oceanic and Atmospheric Administration (NOAA)<sup>52</sup> for the period of June 2010 to November 2013.

### Geochemical analysis and modeling:

DOC was measured on filtered samples by high-temperature combustion using a Shimadzu TOC-V organic carbon analyzer and established methods<sup>53</sup>. DOC concentrations were calculated from the mean of 3 injections having a coefficient of variance <2% and fit to a 6-point calibration curve. An internal standard was analyzed periodically to assess baseline drift. The total precision between independent measurements was <5%. Geochemical measurements including,  $\text{SO}_4^{2-}$ ,  $\text{SiO}_2$ ,  $\text{Cl}^-$ ,  $\text{Ca}^{2+}$ ,  $\text{Mg}^{2+}$ ,  $\text{Na}^+$ , and  $\text{K}^+$  were obtained from filtered water samples (see supplemental methods).

Daily discharge and DOC fluxes were calculated using the FORTRAN Load Estimator (LOADEST) program<sup>54</sup> and then summed to calculate annual loads for year 1 (August 2011 to July 2012) and year 2 (August 2012 to July 2013). The calibration equation was derived using the Adjusted Maximum Likelihood Estimator (AMLE) and the regression model number was set to default (MODNO = 0), allowing for selection of the best model based on Akaike Information Criteria. The validity of the model was verified from the output of the  $R^2$  of the AMLE, residuals data, and the serial correlation of residuals including confirmation that the residuals were normally distributed according to previous methods<sup>55</sup>.

Solid phase extraction:

Filtered water samples were extracted for FT-ICR MS analysis with Varian Bond Elut PPL columns (25 mg) as described by Dittmar et al.<sup>56</sup> Briefly, columns were rinsed with Milli-Q water acidified to pH 2 with concentrated HCl, conditioned with methanol, and rinsed once more with pH 2 Milli-Q water. Water samples (~20 mL) acidified to pH 2 were then passed through the columns via gravity. Columns were then rinsed with pH 2 Milli-Q water, dried under argon gas, and the DOM was eluted with high-purity methanol into precombusted glass vials. The vials were stored in the dark at -20° C prior to FT-ICR MS analysis.

Fourier transform-ion cyclotron resonance mass spectrometry (FT-ICR MS):

The DOM-methanol extracts were diluted using Milli-Q water and methanol to a final DOC concentration of  $5 \text{ mg C L}^{-1}$  and a methanol:water volume ratio of 1:1 then continuously infused into the electrospray ionization source of a Bruker Solarix 15 T FT-ICR MS instrument (University of Oldenburg, Germany). The flow rate was  $120 \mu\text{L hr}^{-1}$  in negative mode and 200 scans were acquired for each sample. Instrument sensitivity was monitored using a standard reference material (NELHA extracted marine DOM). Raw mass spectra were calibrated using a reference mass list to mass accuracy of less than 0.1 ppm. Only peaks above the method detection limit were considered<sup>57</sup>.

Masslists were aligned according to m/z. Formulae containing  $\text{C}_{2-60}$ ,  $\text{H}_{2-122}$ ,  $\text{O}_{1-34}$ ,  $\text{N}_{0-4}$ ,  $\text{S}_{0-2}$ , and  $\text{P}_{0-1}$  were then assigned to matched mass spectral peaks using in-house developed software according to previously published rules<sup>10</sup>. The spectra were then blank corrected by removing contamination peaks found in PPL extracted methanol blanks. Chemical properties including the stoichiometric ratios of heteroatoms to carbon (e.g. H/C, O/C, N/C, etc.), modified aromaticity index ( $\text{AI}_{\text{mod}}$ )<sup>58,59</sup> and average carbon oxidation state ( $\text{C}_{\text{OX}}$ )<sup>60</sup> were calculated using abundance-weighted elemental counts from the

assigned molecular formulae. The abundance-weighted average of formulae within the Island of Stability (IOS) was defined as formulae with  $1.04 < H/C < 1.3$ ,  $0.42 < O/C < 0.62$ ,  $332 < M/Z < 338$ , and  $446 < M/Z < 548$  after Lechtenfeld et al.<sup>11</sup>

#### Statistical methods:

Post processing and statistical analysis of the formulae were conducted using Microsoft Excel and R with the ggplot2 package<sup>61</sup>. Differences in chemical compositions between years were evaluated by performing a two-sample T test at the  $\alpha=0.05$  significance level. The percent dissimilarity between all samples was calculated using a Jaccard matrix with the Jaccard index ranging from 0 to 100 where 0 is identical and 100 is completely dissimilar. Additionally, formulae common in all samples were pooled together and compared to each individual using the Jaccard index with their resulting dissimilarities fit to a loess regression through time.

Spearman correlations between the relative abundance of all Amazon River formulae and ONI and SOI values from a 0 to 12-month lag were calculated using the psych package in R<sup>62</sup>. Significantly correlated formulae between each lagged index were only considered if they had a false discovery rate corrected  $p$ -value ( $p < 0.05$ )<sup>63</sup>.

#### Data availability:

The authors declare that all data supporting the results of this study other than non-categorized FT-ICR MS data are available within the manuscript and its supplemental files. Non-categorized FT-ICR MS formulae data are available from the corresponding author upon request.

## Declarations

#### Acknowledgements:

The authors would like to thank Ina Ulber and Ekaterina Bulygina for assistance with sample processing, and a network of collaborators in Santarem, Brazil for their local expertise and logistical assistance. This work was partially supported by National Science Foundation grant OCE-1464396 to R.G.M.S. and funding from the Harbourton Foundation to R.G.M.S., R.M.H., and B.P.E.

#### Author contributions:

R.G.M.S., A.S., J.M.S.M., R.M.H. and B.P.E. conceived the study. A.S., R.M.H., J.M.S.M., M.M. and R.G.M.S. carried out the fieldwork and sample collection. A.S., T.Drake., J.M.S.M., H.O., T.Dittmar, B.P.E., M.M. and

R.G.M.S. performed sample analyses. M.R.K. conducted data analysis and wrote the manuscript with significant contributions from A.S., T.Drake, J.M.S.M., R.M.H., H.O., T. Dittmar, B.P.E. and R.G.M.S.

### Competing interests:

The authors declare no competing interests.

## References

1. Cole, J. J. et al. Plumbing the global carbon cycle: integrating inland waters into the terrestrial carbon budget. *Ecosystems* **10**, 172–185 (2007).
2. Battin, T. J. et al. The boundless carbon cycle. *Nature Geoscience* **2**, 598–60 (2009).
3. Tranvik, L. J. et al. Lakes and reservoirs as regulators of carbon cycling and climate. *Limnology and Oceanography* **54**, 2298–2314 (2009).
4. Drake, T. W., Raymond, P. A., & Spencer, R. G. Terrestrial carbon inputs to inland waters: A current synthesis of estimates and uncertainty. *Limnology and Oceanography Letters* **3**, 132–142 (2018).
5. Amon, R. M. & Benner, R. Bacterial utilization of different size classes of dissolved organic matter. *Limnology and Oceanography* **41**, 41–51 (1996).
6. Amon, R. M. W. & Benner, R. Photochemical and microbial consumption of dissolved organic carbon and dissolved oxygen in the Amazon River system. *Geochimica et Cosmochimica Acta* **60**, 1783–1792 (1996).
7. Aufdenkampe, A. K., Hedges, J. I., Richey, J. E., Krusche, A. V., & Llerena, C. A. Sorptive fractionation of dissolved organic nitrogen and amino acids onto fine sediments within the Amazon Basin. *Limnology and Oceanography* **46**, 1921–1935 (2001).
8. Spencer, R. G. et al. Chromophoric dissolved organic matter export from US rivers. *Geophysical Research Letters* **40**, 1575–1579 (2013).
9. Kellerman, A. M. et al. Unifying concepts linking dissolved organic matter composition to persistence in aquatic ecosystems. *Environmental Science & Technology* **52**, 2538–2548 (2018).
10. Stubbins, A. et al. Illuminated darkness: Molecular signatures of Congo River dissolved organic matter and its photochemical alteration as revealed by ultrahigh precision mass spectrometry. *Limnology and Oceanography* **55**, 1467–1477 (2010).
11. Lechtenfeld, O. J. et al. Molecular transformation and degradation of refractory dissolved organic matter in the Atlantic and Southern Ocean. *Geochimica et Cosmochimica Acta* **126**, 321–337 (2014).
12. Gonsior, M. et al. Chemodiversity of dissolved organic matter in the Amazon Basin. *Biogeosciences* **13**, 4279–4290 (2016).
13. Riedel, T. et al. Molecular signatures of biogeochemical transformations in dissolved organic matter from ten world rivers. *Frontiers in Earth Science* **4**, 85 (2016).
14. Vannote, R. L., Minshall, G. W., Cummins, K. W., Sedell, J. R., & Cushing, C. E. The river continuum concept. *Canadian journal of fisheries and aquatic sciences* **37**, 130–137 (1980).

15. Hedges, J. I., Keil, R. G., & Benner, R. What happens to terrestrial organic matter in the ocean?. *Organic geochemistry* **27**, 195–212 (1997).
16. Aufdenkampe, A. K. Riverine coupling of biogeochemical cycles between land, oceans, and atmosphere. *Frontiers in Ecology and the Environment* **9**, 53–60 (2011).
17. Richey, J. E. Biogeochemistry of carbon in the Amazon River. *Limnology and Oceanography* **35**, 352–371 (1990).
18. Moreira-Turcq, P., Seyler, P., Guyot, J. L., & Etcheber, H. Exportation of organic carbon from the Amazon River and its main tributaries. *Hydrological Processes* **17**, 1329–1344 (2003).
19. Raymond, P. A. & Spencer, R. G. Riverine DOM. In *Biogeochemistry of marine dissolved organic matter* (Academic Press, Cambridge, 2015).
20. Devol, A. H., Forsberg, B. R., Richey, J. E., & Pimentel, T. P. Seasonal variation in chemical distributions in the Amazon (Solimoes) River: a multiyear time series. *Global Biogeochemical Cycles* **9**, 307–328 (1995).
21. Moquet, J. S. et al. Amazon River dissolved load: temporal dynamics and annual budget from the Andes to the ocean. *Environmental Science and Pollution Research* **23**, 11405–11429 (2016).
22. Benner, R., Opsahl, S., Chin-Leo, G., Richey, J. E., & Forsberg, B. R. Bacterial carbon metabolism in the Amazon River system. *Limnology and Oceanography* **40**, 1262–1270 (1995).
23. Aufdenkampe, A. K. et al. Organic matter in the Peruvian headwaters of the Amazon: Compositional evolution from the Andes to the lowland Amazon mainstem. *Organic Geochemistry* **38**, 337–364 (2007).
24. Ward, N. D. et al. Degradation of terrestrially derived macromolecules in the Amazon River. *Nature Geoscience* **6**, 530–533 (2013).
25. Seidel, M. et al. Seasonal and spatial variability of dissolved organic matter composition in the lower Amazon River. *Biogeochemistry* **131**, 281–302 (2016).
26. Medeiros, P. M. et al. Fate of the Amazon River dissolved organic matter in the tropical Atlantic Ocean. *Global Biogeochemical Cycles* **29**, 677–690 (2015).
27. Seidel, M. et al. Molecular-level changes of dissolved organic matter along the Amazon River-to-ocean continuum. *Marine Chemistry* **177**, 218–231 (2015).
28. Quay, P. D. et al. Carbon cycling in the Amazon River: implications from the <sup>13</sup>C compositions of particles and solutes. *Limnology and Oceanography* **37**, 857–871 (1992).
29. Richey, J. E., Melack, J. M., Aufdenkampe, A. K., Ballester, V. M., & Hess, L. L. Outgassing from Amazonian rivers and wetlands as a large tropical source of atmospheric CO<sub>2</sub>. *Nature* **416**, 617–620 (2002).
30. Sawakuchi, H. O. et al. Carbon dioxide emissions along the lower Amazon River. *Frontiers in Marine Science* **4**, 76 (2017).
31. D’Andrilli, J., Junker, J. R., Smith, H. J., Scholl, E. A., & Foreman, C. M. DOM composition alters ecosystem function during microbial processing of isolated sources. *Biogeochemistry* **142**, 281–298

- (2019).
32. Valle, J. et al. Extensive processing of sediment pore water dissolved organic matter during anoxic incubation as observed by high-field mass spectrometry (FTICR-MS). *Water Research* **129**, 252–263 (2018).
  33. Mayorga, E. et al. Young organic matter as a source of carbon dioxide outgassing from Amazonian rivers. *Nature* **436**, 538–541 (2005).
  34. Foley, J. A., Botta, A., Coe, M. T., & Costa, M. H. El Niño–Southern oscillation and the climate, ecosystems and rivers of Amazonia. *Global Biogeochemical Cycles* **16**, 79 (2002).
  35. Ronchail, J. et al. Discharge variability within the Amazon basin. *Climate variability and Change Hydrological Impacts. IAHS Publ* **296**, 21–29 (2005).
  36. Cai, W. et al. ENSO and greenhouse warming. *Nature Climate Change* **5**, 849–859 (2015).
  37. Widlansky, M. J., Timmermann, A., & Cai, W. Future extreme sea level seesaws in the tropical Pacific. *Science Advances* **1**, e1500560 (2015).
  38. Espinoza, J. C. et al. The major floods in the Amazonas River and tributaries (Western Amazon basin) during the 1970–2012 period: A focus on the 2012 flood. *Journal of Hydrometeorology* **14**, 1000–1008 (2013).
  39. Marengo, J. A. et al. Two contrasting severe seasonal extremes in tropical South America in 2012: flood in Amazonia and drought in northeast Brazil. *Journal of Climate* **26**, 9137–9154 (2013).
  40. Richey, J. E., Nobre, C., & Deser, C. Amazon River discharge and climate variability: 1903 to 1985. *Science* **246**, 101–103 (1989).
  41. Hedges, J. I. et al. Origins and processing of organic matter in the Amazon River as indicated by carbohydrates and amino acids. *Limnology and Oceanography* **39**, 743–761 (1994).
  42. Rose, L. A., Karwan, D. L., & Godsey, S. E. Concentration–discharge relationships describe solute and sediment mobilization, reaction, and transport at event and longer timescales. *Hydrological Processes* **32**, 2829–2844 (2018).
  43. D'Andrilli, J., Cooper, W. T., Foreman, C. M., & Marshall, A. G. An ultrahigh-resolution mass spectrometry index to estimate natural organic matter lability. *Rapid Communications in Mass Spectrometry* **29**, 2385–2401 (2015).
  44. Mann, P. J. et al. The biogeochemistry of carbon across a gradient of streams and rivers within the Congo Basin. *Journal of Geophysical Research: Biogeosciences* **119**, 687–702 (2014).
  45. Spencer, R. G., Aiken, G. R., Wickland, K. P., Striegl, R. G., & Hernes, P. J. Seasonal and spatial variability in dissolved organic matter quantity and composition from the Yukon River basin, Alaska. *Global Biogeochemical Cycles* **22**, 1–13 (2008).
  46. Johnston, S. E. et al. Flux and seasonality of dissolved organic matter from the Northern Dvina (Severnaya Dvina) River, Russia. *Journal of Geophysical Research: Biogeosciences* **123**, 1041–1056 (2018).

47. McLaughlin, C., & Kaplan, L. A. Biological lability of dissolved organic carbon in stream water and contributing terrestrial sources. *Freshwater Science* **32**, 1219–1230 (2013).
48. Wagner, S. et al. Molecular hysteresis: hydrologically driven changes in riverine dissolved organic matter chemistry during a storm event. *Journal of Geophysical Research: Biogeosciences* **124**, 759–774 (2019).
49. Pérez, M. A., Moreira-Turcq, P., Gallard, H., Allard, T., & Benedetti, M. F. Dissolved organic matter dynamic in the Amazon basin: sorption by mineral surfaces. *Chemical Geology* **286**, 158–168 (2011).
50. Remington, S., Krusche, A., & Richey, J. Effects of DOM photochemistry on bacterial metabolism and CO<sub>2</sub> evasion during falling water in a humic and a whitewater river in the Brazilian Amazon. *Biogeochemistry* **105**, 185–200 (2011).

## Figures

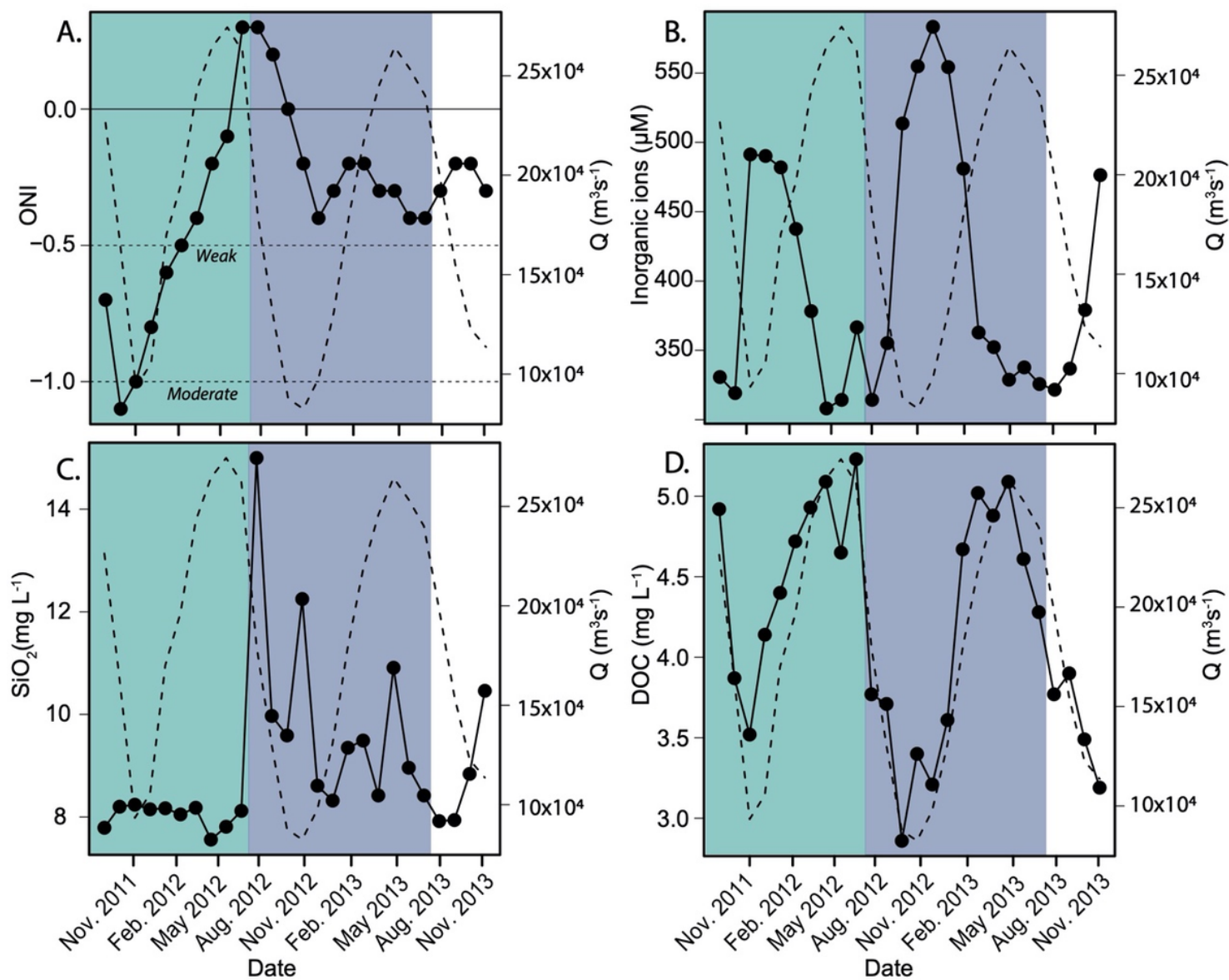


**Figure 1**

(A) Line plot of the Oceanic Niño Index (ONI) during the study period with a weak La Niña event in the region of -0.5 to -1.0 and a moderate La Niña in the region of -1.0 to -1.5. Line plots of (B) major inorganic ions ( $\text{Cl}^-$ ,  $\text{SO}_4^{2-}$ ,  $\text{Ca}^{2+}$ ,  $\text{Mg}^{2+}$ ,  $\text{Na}^+$ ,  $\text{K}^+$ ), (C)  $\text{SiO}_2$  and (D) DOC measured at Óbidos during the study period. Discharge ( $Q$ ) is indicated by the dashed line and study periods are divided into the La Niña year (August 2011 to July 2012; green) and the normal year (August 2012 to July 2013; blue).

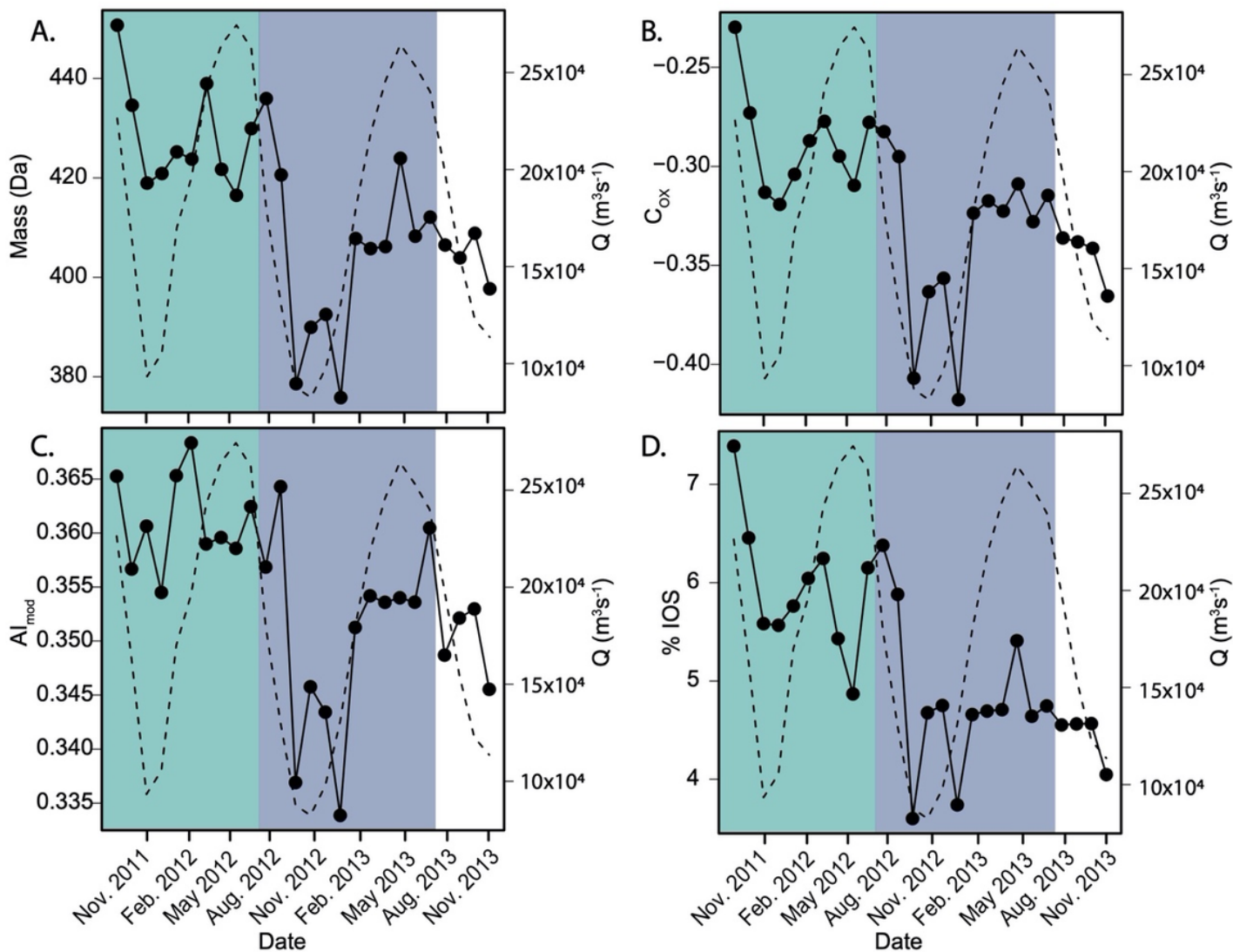


**Figure 2**

Line plots of DOM properties from Óbidos during the study period including (A) average mass, (B) average carbon oxidation state (COX), (C), average modified aromaticity index (Al<sub>mod</sub>) and (D) percent Island of Stability (IOS). Discharge ( $Q$ ) is indicated by the dashed line and study periods are divided into the La Niña year (August 2011 to July 2012; green) and the normal year (August 2012 to July 2013; blue).

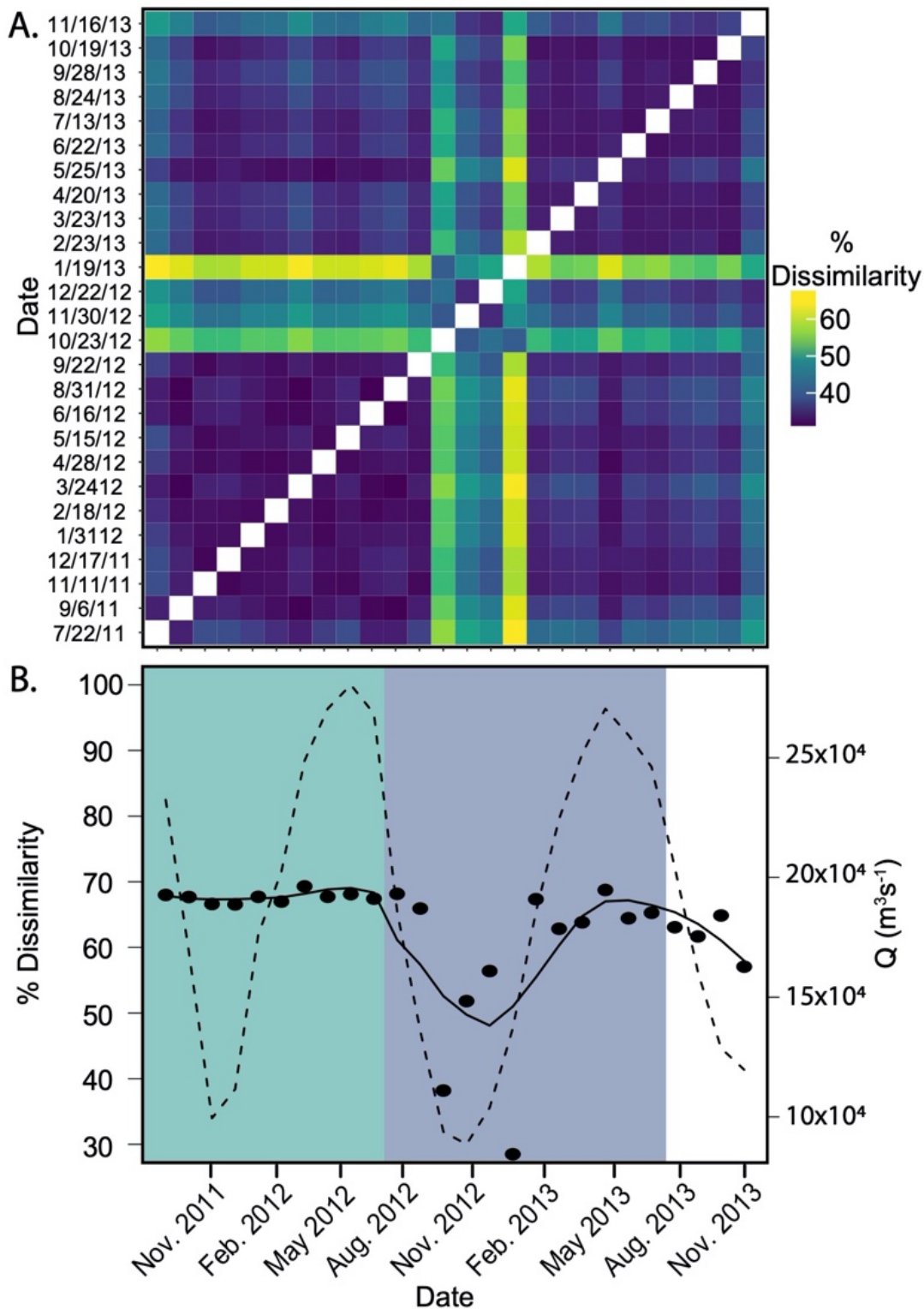


**Figure 3**

(A) Jaccard dissimilarity matrix of Amazon DOM during the study period. (B) The percent dissimilarity between each DOM sample and the group of molecules common across all Amazon samples with a fitted loess regression (solid black line). Discharge ( $Q$ ) is indicated by the dashed line and study periods are divided into the La Niña year (August 2011 to July 2012; green) and the normal year (August 2012 to July 2013; blue).

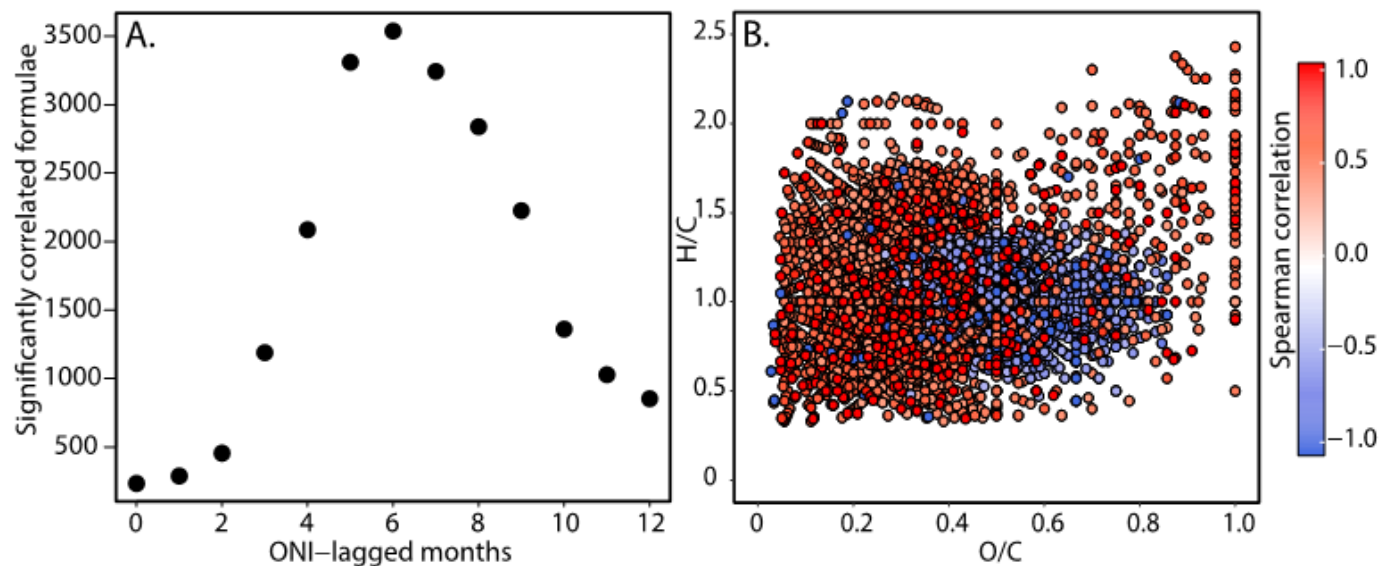


**Figure 4**

(A) Total number of significantly correlated molecular formulae with ONI values lagging from 0 to 12 months. (B) van Krevelen diagram of formulae correlated with ONI values from a 6-month lag period. Red points are positively correlated with ONI values while blue points are negatively correlated with ONI values.

## Supplementary Files

This is a list of supplementary files associated with this preprint. Click to download.

- [Arrhythmia in the Amazon SI081020.docx](#)